URSI AP-RASC, Sydney, Australia, 17 – 22 August 2025

Investigating the Properties of Type III Radio Bursts Using Superposed Epoch Analysis

Huei-Wen Siao(1), Ya-Hui Yang* (2,3)
(1) Central Weather Administration, Taipei, Taiwan
(2) Department of Space Science and Engineering, National Central University, Taoyuan, Taiwan
(3) Center for Astronautical Physics and Engineering, National Central University, Taoyuan, Taiwan

Abstract

Type III radio bursts are the most commonly observed classification of solar radio bursts, characterized by relatively high flux intensity and a rapid frequency drift over time. Analyzing type III radio bursts can serve as a powerful remote sensing diagnostic tool for studying accelerated electron beams and the ambient plasma medium, thereby expanding the potential for monitoring and forecasting space weather. However, there are still some perplexities regarding the characteristics and mechanisms that need to be clarified. In this study, there are 90 type III radio bursts are evaluated with quantitative analysis between Orbit 1 and Orbit 8 Parker Solar Probe (PSP) during periods of high temporal resolution. The application of Superposed Epoch Analysis (SEA) effectively demonstrates that the polarized signal predominantly emerges before or at zero epoch time. Additionally, the classification of polarized type III radio bursts into different pattern categories, which designed in this study, reveals distinct polarized signal signatures and decay times. The aim of this study is to explore the potential relationship between the properties of type III radio bursts.

1. Introduction

Solar Type III radio bursts, characterized by a fast drift from high- to low-frequency in a dynamic spectrum, are the most common and intense category of solar radio bursts [1]. Typically, Type III bursts are regarded as remote sensing diagnostic tools for both accelerated electron beams and the space plasma through which they propagate [2].

Recent studies using observations from Parker Solar Probe (PSP), a new NASA spacecraft mission, have significantly advanced our understanding of type III radio bursts and solar wind density fluctuations. Pulupa et al. [3] showed the first analysis for the polarization properties of type III radio bursts during PSP's second encounter. Jebaraj et al. [4] reported the first detailed observations of fundamental-harmonic pairs in hectokilometric wavelengths, revealing that these characteristic pairs are more easily observed in the majority of type III bursts during close encounters. Krupar et al. [5] analyzed the decay times of type III bursts from 1 to 10 MHz and observed a significant deviation in power-law slope above 1 MHz compared to previous measurements. They predicted relative density fluctuations at the effective turbulence scale length would range from 0.22 to 0.09 between 2.5 and 14 $R_\odot$, with in-situ measurements at 35.7 $R_\odot$ displaying good agreement with previous predictions. Kontar et al. [6] developed an anisotropic density turbulence model, which was compared with multiple observations, including those from PSP, spanning distances from 0.1 $R_\odot$ to 1 AU. Their findings revealed a broad maximum in density fluctuations occurring between 4 and 7 $R_\odot$.

This study applies the Superposed Epoch Analysis (SEA) to examine the polarization properties and decay times of solar type III radio bursts observed by the PSP spacecraft, with the objective of identifying potential relationships.

2. Methodology

In this study, we analyzed 90 type III radio bursts, of which 49 exhibited clear circular polarization signals, while the remaining 41 displayed less prominent circular polarization. These events were observed between Orbit 1 and Orbit 8 of PSP during periods of high temporal resolution (from 2019 April 3 to 2021 May 3). The radio observations of Parker Solar Probe (PSP) are processed using the Radio Frequency Spectrometer (RFS) [7], which is the highest-frequency component of the FIELDS suite, consists of a dual-channel receiver and spectrometer within a bandwidth between 10 kHz and 19.2 MHz. The data reduction of RFS is conducted in two sub-bandwidths: the High Frequency Receiver (HFR), covering frequencies from 1.3 to 19.2 MHz, and the Low Frequency Receiver (LFR), spanning 10.5 kHz to 1.7 MHz. For this study, we initially derived flux density (S, W/m^{2}Hz) utilizing the relationship with power spectral density (P, V^2/Hz) as detailed in the equation denoted as [7]:

$$\mathrm{P} = \mathrm{S} \times \mathrm{Z}_0 \mathrm{L}_{\mathrm{eff}}^2 \Gamma^2. \tag{1}$$

Z_0 represents the impedance of free space, L_{eff} is the effective antenna length, and Γ denotes the capacitive gain factor. The unit of flux density is expressed in solar flux unit (sfu = 10^{-22} W/m^{2}Hz) in this study. For circular polarization, we derived the Stoke parameters, Stoke I and Stoke V from Pulupa et al. (2020), to define the degree of circular polarization (DCP), namely the ratio of Stokes V to I. Figure 1 presents three examples with the signatures of total flux intensity and circular polarization. It is evident that the patterns of circular polarization signals are very different for each other although their total intensity signals seem to be similar.

2.1. Pattern Category

To conduct a more detailed case study analysis, we classified the selected circular polarization signal patterns into two categories, following the criteria outlined in [8]. These categories were manually identified as "Single Polarization Signature" and "Fuzzy Polarization Signature" and "Less Polarization Pattern". "Single Polarization Signature" is that the DCP values within the chosen region are higher dramatically, continue for a short time and constant with frequency. "Fuzzy Polarization Signature" describes cases where the DCP values within the chosen region are smoother, continue for a while and vary with frequency. The examples of two categories are shown on Figure 1.

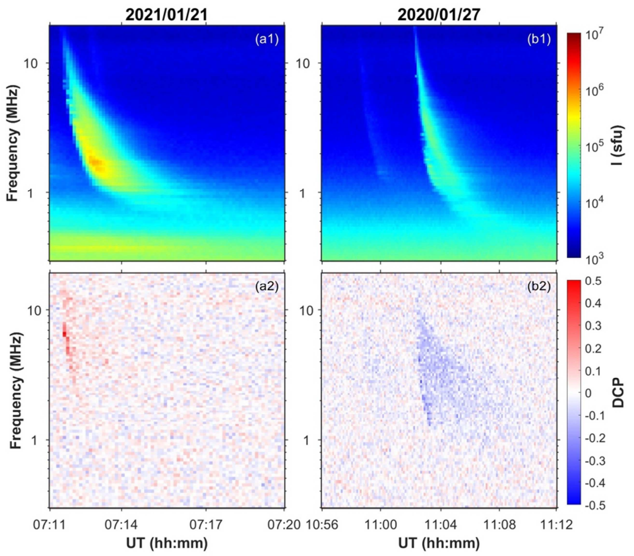

Figure 1. Example type III radio bursts displaying dynamic spectra (panels (a1) and (b1)) in Stoke I and the polarization map (panels (a2) and (b2)) in DCP. There are three circular polarized situations, including single line pattern (panel a2) and fuzzy pattern (panel b2).

2.2. Superposed Epoch Analysis (SEA)

According to earlier literatures, the time profile of type III radio bursts is considered to result from the convolution of plasma wave excitation and damping processes. Specifically, it is influenced by the instability growth driven by the evolution of the accelerated electron beam, as well as the damping effects imposed by variations in the background plasma [9]. In this study, we calculated the exponential decay time τ_d, by measuring the duration from the peak intensity to the half-power level [5]. Besides, we applied the Superposed Epoch Analysis (SEA) to find out the possible relationship between different circular polarization patterns. SEA is a widely used data analysis method, frequently employed to examine periodicities or temporal correlations within time series data [10]. Currently, SEA has applied in extensive applications, including solar-terrestrial environment, space science, and atmospheric science [11]. In this paper, SEA is applied to analyze the total intensity and circular polarized signals of type III radio bursts. SEA needs to define "Epoch time", which represents a specific occurrence time in the time series, which are determined by selecting the peak of total intensity for the chosen type III radio bursts in this study. The analysis considers a time window spanning 10 minutes before and 20 minutes after the peak of the total intensity, resulting in a total time series duration of 30 minutes. Subsequently, the time series data of type III radio bursts were synchronized based on "Epoch time". Following this, the synchronized time series were analyzed to calculate the superposed median and superposed mean profiles, which served to represent the temporal trends across the distinct categories. The total intensity was classified into three categories based on the circular polarized signal patterns observed in the selected type III radio bursts: Single Polarization Signature and Fuzzy Polarization Signature. Notably, the analysis of total intensity and circular polarization was only restricted to the two categories: Single Polarization Signature and Fuzzy Polarization Signature. The reason is that the selected type III radio bursts in these categories met the circular polarization criteria established in the Section 2.1.

3. Results

Figure 2 shows the SEA results of total intensity for five specific frequencies (0.61, 1.01, 5.03, 10.02 and 15.48 MHz) with two different polarization signal patterns. Each gray line in the figure represents the total flux intensity profile of Type III radio bursts, with 33 cases corresponding to the Single Polarization Signature and 16 instances corresponding to the Fuzzy Polarization Signature. The purple line corresponds to the superposed mean profile, while the orange solid line represents the superposed median profile across all instances. In the SEA results of the total intensity signal, the superposed median profile exhibits less sensitivity to the influence of peak values from individual events at different time points compared to the superposed mean profile. This characteristic of the superposed median profile aligns more closely with the overall trend in the total intensity of type III radio burst. Furthermore, the duration over which the superposed median profile returns from its peak value to the background level shows a gradual increase as the frequency decreases.

Figure 3 displays the SEA results with two different polarization signal patterns with same methods and formats as in Figure 2. In the SEA results of the polarized signal, the superposed mean profile, represented by the orange line in Figure 3, proves to be more effective in capturing the overall trend for type III polarized signal profile. Additionally, frequencies exceeding 1 MHz exhibit more prominent peaks at zero epoch time.

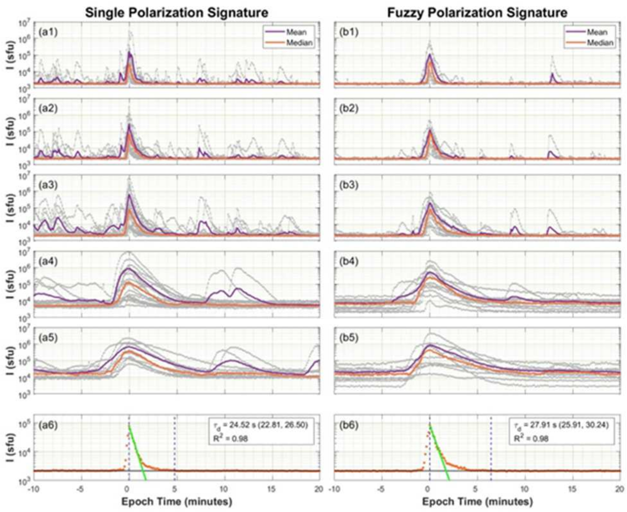

Figure 2. The light curves of total flux intensity with superposed epoch analysis for three different polarization signal patterns: Single, Fuzzy, and Less circular polarization. From row (a1) to (a5), (b1) to (b5), and (c1) to (c5) fixed five frequency channels with 15.48, 10.02, 5.03, 1.01, and 0.61 MHz. The grey line is the time profile for each type III signal around the epoch time. Purple line is mean curve and orange line is median curve. For the row (a6), (b6) and (c6) black line is the median value in a given time interval. Blue dashed lines show peak Stoke I and the last points above the median value. The green line denotes the results of the decay time τ_d.

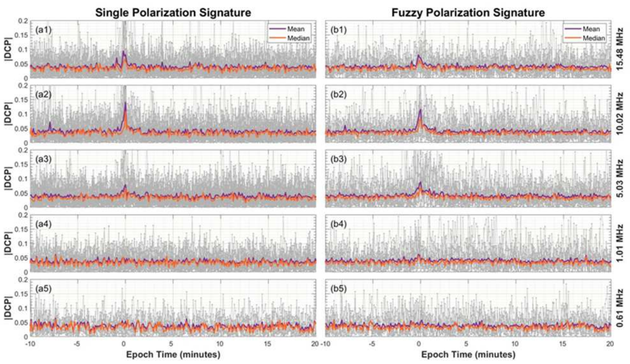

Figure 3. The light curves of circular polarized signal with superposed epoch analysis for three different polarization signal patterns: Single, Fuzzy, and Less circular polarization. From row (a1) to (a5) and from (b1) to (b5) fixed five frequency channels with 15.48, 10.02, 5.03, 1.01, and 0.61 MHz. The grey line is the time profile for each type III signal around the epoch time. Purple line is mean curve and orange line is median curve.

Figure 4 presents the dynamic spectra of SEA results categorized by different circular polarized categories. As shown in Figure 4 (a2), the results for the Single Polarization Signature indicate that most of the larger DCP values occur at or before zero epoch time. This implies that following the peak total intensity, the circular polarized signal is notably absent within type III radio bursts, a trend also reported by [3]. In contrast, Figure 4 (b2) illustrates that the Fuzzy Polarization Signature category exhibits larger DCP values after zero epoch time and a tendency indicating a gradual increase in duration as the frequency decreases.

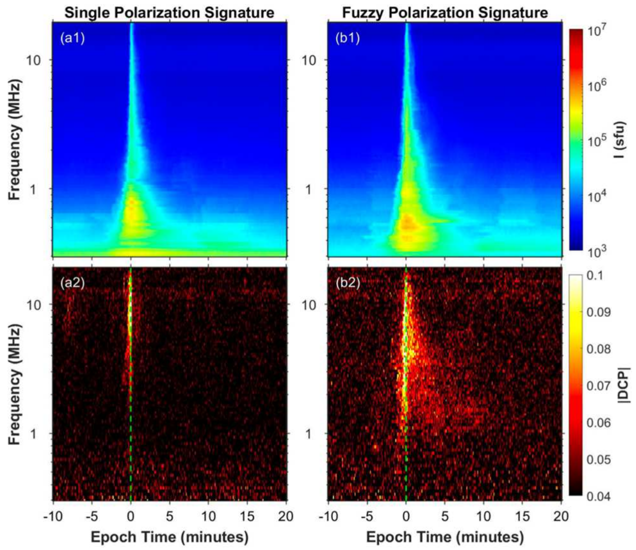

Figure 4. The dynamic spectrum of SEA results with different circular polarized categories. Figure (a1) and (a2) depict results for the Single Polarization Signature, while (b1) and (b2) represent the Fuzzy Polarization Signature. The dashed green lines on Figure (a2) and (b2) note the zero epoch time.

4. Summary

The objectives of the present study are to investigate the polarized type III radio bursts by the radio observations from FIELIDS/RFS in high temporal resolution on PSP in its first eight orbits (2019 April 3-2021 May 3). The main finding can be summarized as follow:

1. The SEA method effectively demonstrates that the polarized signal predominantly emerges before or at zero epoch time.
2. In the Single Polarization Signature category, the polarized signal is absent after zero epoch time. Conversely, for the Fuzzy Polarization Signature category, the polarized signal exhibits a longer duration as it appears after zero epoch time.

Overall, PSP provides novel insights into understanding of properties of the solar radio bursts observed in the inner heliosphere. While some of the findings align with observations made at 1 AU, the current study bridges the gap in space-based polarization observations, revealing only the tip of the iceberg concerning solar radio emissions. Further research could involve a comprehensive assessment of in-situ electron measurements from PSP, in conjunction with multi-observational data, to evaluate additional observed properties of type III radio bursts as well as to identify radio sources through imaging techniques. Such studies could enable type III radio bursts as remote sensing diagnostic tools for the energetic electron beams and solar system plasma they propagate through, offering valuable insights to improve the monitoring and forecasting of space weather.

5. Acknowledgements

Parker Solar Probe was designed, built, and is now operated by the Johns Hopkins Applied Physics Laboratory as part of NASA's Living with a Star (LWS) program (contract NNN06AA01C). Support from the LWS management and technical team has played a critical role in the success of the Parker Solar Probe mission. Thanks to the FIELDS team for providing data (PI: Stuart D. Bale, UC Berkeley), which are publicly available at http://fields.ssl.berkeley.edu/data/. This work is supported by the Ministry of Science and Technology of the R.O.C. under grants MOST 110-2111-M- 008-019 and NSTC 113-2111-M-008-020.

References

[1] J. P. Wild and L. L. McCready, "Observations of the Spectrum of High-Intensity Solar Radiation at Metre Wavelengths. I. The Apparatus and Spectral Types of Solar Burst Observed," *Australian Journal of Scientific Research A Physical Sciences*, vol. 3, p. 387, September 01, 1950 1950, doi: 10.1071/ch9500387.

[2] H. A. S. Reid and H. Ratcliffe, "A review of solar type III radio bursts," *Research in Astronomy and Astrophysics,* vol. 14, no. 7, pp. 773-804, 2014, doi: 10.1088/1674-4527/14/7/003.

[3] M. Pulupa *et al.*, "Statistics and Polarization of Type III Radio Bursts Observed in the Inner Heliosphere," *The Astrophysical Journal Supplement Series,* vol. 246, no. 2, 2020, doi: 10.3847/1538-4365/ab5dc0.

[4] I. C. Jebaraj, V. Krasnoselskikh, M. Pulupa, J. Magdalenic, and S. D. Bale, "Fundamental–Harmonic Pairs of Interplanetary Type III Radio Bursts," *The Astrophysical Journal Letters,* vol. 955, no. 1, 2023, doi: 10.3847/2041-8213/acf857.

[5] V. Krupar *et al.*, "Density Fluctuations in the Solar Wind Based on Type III Radio Bursts Observed by Parker Solar Probe," *The Astrophysical Journal Supplement Series,* vol. 246, no. 2, 2020, doi: 10.3847/1538-4365/ab65bd.

[6] E. P. Kontar *et al.*, "An Anisotropic Density Turbulence Model from the Sun to 1 au Derived from Radio Observations," *The Astrophysical Journal,* vol. 956, no. 2, 2023, doi: 10.3847/1538-4357/acf6c1.

[7] M. Pulupa *et al.*, "The Solar Probe Plus Radio Frequency Spectrometer: Measurement requirements, analog design, and digital signal processing," *Journal of Geophysical Research (Space Physics),* vol. 122, pp. 2836-2854, March 01, 2017 2017, doi: 10.1002/2016ja023345.

[8] H.-W. Siao and Y.-H. Yang, "Characteristics of Circular Polarized Type III Radio Bursts in the Inner Heliosphere," in *2023 XXXVth General Assembly and Scientific Symposium of the International Union of Radio Science (URSI GASS)*, Sapporo, Japan, October 01, 2023 2023, p. 310, doi: 10.23919/ursigass57860.2023.10265308. [Online]. Available: https://ui.adsabs.harvard.edu/abs/2023ursi.confE.310S

[9] A. O. Benz, *Plasma astrophysics [electronic resource] : kinetic processes in solar and stellar coronae / by Arnold O. Benz*, 2nd ed. (Astrophysics and space science library ; v. 279). Dordrecht ;: Kluwer Academic Publishers, 2002.

[10] C. Chree, "Some Phenomena of Sunspots and of Terrestrial Magnetism at Kew Observatory," *Philosophical Transactions of the Royal Society of London Series A,* vol. 212, pp. 75-116, January 01, 1913 1913, doi: 10.1098/rsta.1913.0003.

[11] Y. P. Singh and Badruddin, "Statistical considerations in superposed epoch analysis and its applications in space research," *Journal of Atmospheric and Solar-Terrestrial Physics,* vol. 68, pp. 803-813, April 01, 2006 2006, doi: 10.1016/j.jastp.2006.01.007.